II. ANALYSIS OF DIII-D EXPERIMENTS (DOE GRANT ER54538)

A. TRANSPORT IN THE EDGE PEDESTAL

(W. M. Stacey and R. J. Groebner)

Theoretical heat conductivities based on analytical representations of neoclassical and ITG modes for the ions and ETG and TEM modes for the electrons have been compared with measured transport rates in the edge pedestal for several DIII-D shots with a wide range of edge parameters. Thermal transport coefficients from the neoclassical, ITG and ETG theories are found to be within at most a factor of 2-3 of values inferred from experiment for most of the discharges considered, as shown in Table 1.

Table 1: Experimental and theoretical thermal conductivities (m^2/s)

Shot	ν_e^*	L_{Ti}/L_{Ti}^{crit}	η_e	$\chi_i^{exp,a}$	χ_i^{NEO}	χ_i^{ITG}	$\chi_e^{exp,a}$	χ_e^{TEM}	χ_e^{ETG}
93045	0.10	0.27	1.03	0.20	0.31(0.67[b])	3.7	0.17	>100	2.4
87085	0.28	0.49	0.96	1.1	0.58(0.93)	2.5	1.4	52	3.6
97979	0.40	0.36	1.27	0.80	0.49(0.54)	1.7	0.48	44	1.6
106005	0.30	0.31	1.29	1.1	0.62(0.76)	1.7	0.57	62	2.8
106012	0.62	0.60	1.20	1.6	0.51(0.67)	0.59	0.73	21	1.5
92976	1.53	0.60	1.43	1.5	0.53(0.84)	0.37	1.3	1.6	1.4
98893	4.86	0.59	1.00	1.0	0.62(0.68)	0.20	0.34	1.7	0.55

[a] Experimental values evaluated assuming $Q_i = Q_e$.
[b] Without orbit squeezing correction.

The edge gradients of these discharges are such that ITG and ETG modes are predicted to be unstable. This finding that ETG modes should be unstable in the edge is consistent with previous observation of $\eta_e \approx 2$ in a large number of discharges in ASDEX Upgrade[1]. Furthermore, the results shown in Fig. 16 of Ref. 2 imply that $\eta_e \approx 1.5$ in a large number of DIII-D discharges.

New expressions for a 'diffusive-pinch' form of particle flux, for calculating an experimental frequency for momentum transfer, and for predicting the density gradient scale length have been derived from momentum balance. The experimental momentum transfer rates are too large by an order of magnitude to be accounted for by atomic physics and convective momentum transfer, but neoclassical gyroviscous theory predicts frequencies comparable to those found experimentally.

The new expression for the density gradient scale length of ion species 'j' is

$$L_{nj}^{-1} = \frac{e_j B_\theta}{n_j m_j \nu_{dj}^* T_j}\left[e_j B_\theta \Gamma_j + M_{\phi j} + n_j e_j E_\phi^A - n_j m_j \nu_{jk}\left(\upsilon_{\phi j} - \upsilon_{\phi k}\right)\right] - \frac{e_j B_\theta}{T_j}\left(f_p^{-1}\upsilon_{\theta j} + \frac{E_r}{B_\theta}\right) - L_{Tj}^{-1} \quad (1)$$

We find that the momentum input (M_φ) and toroidal electric field (E_φ) contributions are negligible and would expect that the friction term can also be neglected. The import of Eq. (1) is then that the pressure gradient scale length is determined by the particle flux (Γ) and momentum transfer rate (ν_d*), by the poloidal rotation, and by the radial electric field, which latter is related to both poloidal and toroidal rotation velocities. Since the temperature gradient scale length is determined by heat transport, the density gradient scale length must adjust to satisfy this momentum balance constraint on the pressure gradient. We expect these transport constraints to govern the pedestal gradient scale lengths between or in the absence of ELMs.

We evaluated an average value of the gradient scale length from Eq. (1) for the main ion species as follows. The momentum transfer frequency was calculated from the neoclassical expression[3] plus the atomic physics and convective momentum transfer frequencies. The radial particle flux was determined from particle balance, and the neutral beam momentum input in the pedestal was calculated directly. The friction term involving the difference in ion and impurity toroidal velocities was assumed to be negligible. The E_φ^A term and the temperature gradient scale length term were evaluated from experimental data. The poloidal velocity was determined by solving coupled Fourier moments of the poloidal momentum balance equation for the poloidal velocities of the ions and impurities and for the sine and cosine components of the ion and impurity density asymmetries which are needed to evaluate the poloidal asymmetry factor needed to evaluate the neoclassical gyroviscous contribution to ν_d*; this calculation is described in detail in Ref. 4. The radial electric field was calculated by summing the toroidal components of the momentum balance equation for the ions and impurities to obtain

$$\frac{E_r}{B_\theta} = \frac{\left\{M_{\phi i} + M_{\phi I}\right\} + n_i m_i \nu_{di}^*\left(P_i^{'} - f_p^{-1}\upsilon_{\theta i}\right) + n_I m_I \nu_{dI}^*\left(P_I^{'} + f_p^{-1}\upsilon_{\theta I}\right)}{n_i m_i \nu_{di}^* + n_I m_I \nu_{dI}^*} \quad (2)$$

and using the theoretical values of v_{di}*and $\upsilon_{\theta i}$ just discussed, together with the experimental value of P_i'. Density gradient scale lengths calculated from Eq. (1) are within a factor of 2 or closer of those measured directly (Thomson scattering), as shown in Table 2, confirming the consistency of the calculation.

Table 2: Density gradient scale lengths

Shot	93045	87085	97979	106005	106012	92976	98893
Exp. L_n	2.8	4.3	3.3	2.7	2.4	6.0	1.5
Calc. L_n	2.7	3.3	2.4	1.9	1.8	3.3	0.8

Perhaps the most significant finding of this investigation is that neoclassical theory appears to provide a reasonable representation of ion transport in the edge pedestal. The neoclassical predictions of both ion thermal conductivity and ion momentum transfer frequency were within a factor of 2-3 or less of the experimental values, and the use of neoclassical momentum transfer frequencies in the calculation of density gradient scale lengths results in a prediction that is within a factor of 2 of the directly measured value.

A paper has been prepared for Physics of Plasmas, and a presentation was made at APS-DPP-03.

1. J. Neuhauser, D. P. Coster, H. U. Farbach, et al., Plasma Phys. Control. Fusion, 44, 855 (2002).
2. R. D. Deranian, R. J. Groebner and D. T. Pham, Phys. Plasmas, 7, 1235 (2000).
3. W. M. Stacey and D. J. Sigmar, Phys. Fluids, 28, 2800 (1985).
4. W. M. Stacey, Phys. Plasmas, 9, 3874 (2002).

B. L-H POWER THRESHOLD

(W. M. Stacey)

It was shown recently[1] that there is a critical, threshold non-radiative heat flux through the plasma edge above which thermal instabilities with short radial wavelengths[2] are stabilized. This critical heat flux can be represented as a threshold power crossing the separatrix

$$P_{thresh} = \frac{5}{4}\Gamma_\perp T\, A_{sep}\left[\sqrt{1+\frac{\left(\chi^0\left(\alpha-\chi^0 k_r^2\right)/\nu\right)}{\left(\frac{5}{4}\frac{\Gamma_\perp}{n}\right)^2}}+1\right] \qquad (1)$$

where $k_r^{-1} \approx$ 1-10 cm is the radial wavelength of the instability, $\chi_0 \approx 0.1 - 1.0$ m^2/s is the background thermal conductivity in the absence of thermal instabilities, $\nu \approx 3/2 - 7/2$ represents the temperature dependence of $\chi_0 \sim T^\nu$, α represents the temperature dependence of the atomic physics cooling terms, $\Gamma\perp$ is the ion flux crossing the separatrix and A_{sep} is the area of the separatrix.

The predicted phenomena[1]--a decrease in the values of both edge temperature gradient scale length and the heat conductivity associated with the thermal instabilities as the power flux approached the threshold value from below and the sharp decrease in both quantities as the threshold was crossed--were suggestive of the low-to-high (L-H) transition in tokamaks. The predicted phenomena as the power flux approached the threshold value from above were similarly suggestive of the H-L back transition.

A first test of this prediction of a threshold heat flux for the H-L back transition against data from DIII-D was recently made[3] for a set of 'density limit' shots in which the density was increased in H-mode discharges by gas fueling until a H-L mode back transition took place. The increasing density produced increasing core radiation and, at constant heating power, decreasing non-radiative power flowing outward across the separatrix. Good agreement was obtained between the predicted and experimental values of the non-radiative power crossing the separatrix at the time of the H-L back transition for a set of shots with high radiative power fraction. We have now made a similar comparison of predicted and measured values of the non-radiative power crossing the separatrix at the time of the L-H transition for a representative set of DIII-D shots in which the radiative power fraction is small at the time of the transition.

Good agreement has been found between the measured non-radiative power crossing the separatrix just prior to a L-H transition and the sum of the predicted threshold powers for thermal instability stabilization in the ion and electron power balances, for a set of shots with core radiative power fractions of 10% or less, as shown in Table 1. The calculation is relatively insensitive to the exact value of k_r^{-1}, χ_0 , or ν in the above ranges.

Table 1 Some DIII-D shots just prior to the L-H transition (R=1.71-1.79m, a=0.6m, κ=1.73-1.89, LSN divertor)

Shot #	Time (ms)	I (MA)	B (T)	P_{NB} (MW)	δ	n_{eped} (e19/m^3)	T_{eped} (eV)	$P_{sep}^{exp,b}$ (MW)	P_{thr}^{c} (MW)
102456	1725	1.4	2.0	2.6	0.73	3.22	95	1.55-1.86	1.54
97979	1900	1.4	2.0	2.0	0.79	2.59	125	1.72-2.04	2.18
92079	2275	1.0	2.1	6.8	0.37	1.28	220	3.99-4.06	4.00
84027	2575	1.3	2.1	1.1	0.32	2.94	144	1.28-1.36	1.13
97979[a]	3250	1.4	2.0	6.5	0.79	6.35	525	4.64-4.96	2.59

[a] well into H-mode phase, not at the L-H transition—control case

[b] experimental non-radiative power across separatrix (range reflects uncertainty in $P_{radcore}$)

[c] prediction of power threshold for stabilization of thermal instabilities

We recall the previous finding[4] that the same power threshold expression predicts values in good agreement with measured non-radiative power crossing the separatrix just prior to a H-L back transition for a set of 'density limit' shots with core radiative power fractions of 20-40%. These findings combine to provide a strong suggestion that stabilization of thermal instabilities in the edge pedestal plays a major role in triggering the L-H transition and that destabilization plays a similar role in triggering the back H-L transition.

Even broader experimental support for the stabilization of thermal instabilities as a trigger mechanism for the L-H transition may be inherent in the recent finding[4] that edge gradients in temperature and pressure may be better control parameters for predicting the L-H transition than the edge values of the temperature or pressure. The temperature and pressure gradients, but not the electron density gradient, all measured in the region in which the H-mode pedestal ultimately formed, were found to increase during the L-mode phase in shots which made a H-mode transition. This is consistent

with the predicted thermal instability stabilization due to increasing temperature gradients as the threshold power is approached that was discussed in Ref. 1.

To put these results in perspective, we note that the L-H transition has been studied experimentally for more than a decade (e.g. Refs. 5-9) and that the reigning paradigm for the L-H transition that has emerged is the suppression of turbulent transport by the sheared ExB flow produced by a sharp gradient in the negative radial electric field just inside the separatrix. Triggering mechanisms previously put forward to account for the creation of this local radial electric field shear include orbit loss[10] and Stringer spin-up[11]. It has been suggested[1] that the reduced transport that occurs when the power threshold of Eq. (1) is exceeded produces a reduced particle flux across the separatrix (supported by D_α measurements) that in turn produces a positive poloidal rotation (as observed) that results via momentum balance in a negative radial electric field. Thus, the thermal instability suppression mechanism[1], the threshold power prediction of which was confirmed in this paper and in Ref. 3, provides another possible explanation for the trigger mechanism for L-H and H-L transitions.

A paper has been prepared for Physics of Plasmas.

1. W. M. Stacey, Phys. Plasmas, 9, 3082 (2002).
2. W. M. Stacey, Phys. Plasmas, 6, 2452 (1999).
3. W. M. Stacey and T. W. Petrie, Phys. Plasmas, 10, 3349 (2003).
4. R. J. Groebner, D. M. Thomas and R. D. Deranian, Phys. Plasmas, 8, 2722 (2001).
5. E. J. Doyle, R. J. Groebner, K. H. Burrell*, et al.*, Phys. Fluids B, 3, 2300 (1991).
6. R. J. Groebner, Phys. Fluids B, 5, 2343 (1993).
7. K. H. Burrell, E. J. Doyle, P. Gohil, *et al*., Phys. Plasmas, 1, 1536 (1994).
8. K. H. Burrell, Phys. Plasmas, 4, 1499 (1997).
9. R. J. Groebner, D. R. Baker, K. H. Burrell, *et al.*, Nucl. Fusion, 41, 1789 (2001).
10. K. C. Shaing and E. C. Crume, Phys. Rev. Lett., 63, 2369 (1989); K. C. Shaing, E. C. Crume and W. A. Houlberg, Phys. Fluid B, 2, 1492 (1990).
11. A. B. Hassam, T. M. Antonsen, J. F. Drake and C. S. Liu, Phys. Rev. Lett., 66, 309 (1991).

C. NEUTRAL TRANSPORT

(J. Mandrekas, W. M. Stacey, R. J. Colchin, T. W. Petrie)

The Transmission/Escape Probability (TEP) 2-D neutral transport code GTNEUT is a computationally efficient alternative to traditional Monte Carlo methods. Recent implementation of a realistic wall reflection model allowed us to analyze DIII-D neutral density measurements and to benchmark GTNEUT against both Monte Carlo and experiment[1].

GTNEUT was recently upgraded with new capabilities which greatly facilitated setting up and performing DIII-D neutral transport simulations. These upgrades included: a) the implementation of a high performance sparse matrix solver for the solution of the

linear system of neutral transport equations, which allows us to run much larger and geometrically detailed problems and b) the development of an interface routine that can prepare the geometric part of the GTNEUT input file (which is the most laborious part) automatically by directly reading EFIT EQDSK files.

To illustrate the capabilities of the upgraded code, we used it to calculate the exhaust rates from the dome and baffle pumps for the DIII-D shot 113026 @ 3000 ms (an upper single null discharge with dRsep ≈ 1.2, part of the AT Divertor Pumping series of experiments). The upper part of the model geometry is shown in Fig.1 (we actually modeled the entire plasma chamber to exercise the code). For the background plasma parameters (electron and ion densities and temperatures) inside the separatrix, we assumed poloidal symmetry and used the values obtained from GAProfiles. For the plasma parameters in the SOL above and below the X-point, we used other experimental data. For the regions where experimental data were unavailable (private flux region and the near-vacuum regions between the first wall and the last open flux surface) we assigned plausible background plasma parameters.

The results of the neutral transport simulations depend on the ion and neutral recycling assumptions. Since no detailed information on the location and magnitude of the recycling sources was available for this shot, our reference simulation assumed in/out symmetry and equal recycling sources from the four wall segments (84, 86, 93, 95) adjacent to the dome and baffle pump entrances (segments 85 and 94) in Fig. 1. This is a reasonable assumption given the flux expansion between the X-point and the strike points and the experimental indication of comparable recycling rates from inside and outside. The magnitude of the recycling sources was based on a crude estimate from the in/out ion flows at the pre-sheath, but the magnitude is not important since the transport problem is linear and we were interested in the ratio of the exhaust rates (the neutral fluxes to segments 85 and 94). For this reference case, $\Gamma_{dome} / \Gamma_{baffle} = 0.88$ was calculated, in quite good agreement with the ratio of measured exhaust rates.

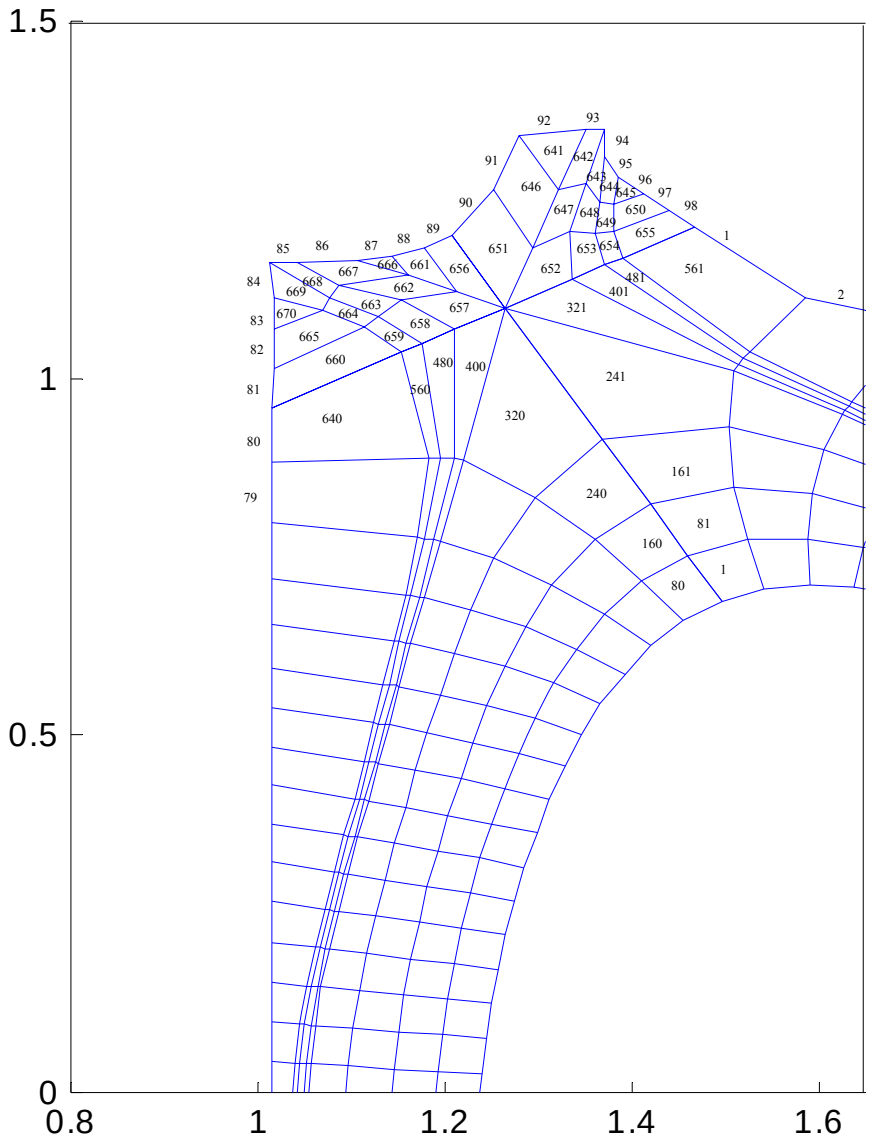

The

Figure 4: Upper part of DIII-D geometry used by GTNEUT for the analysis of DIII-D shot 113026 @ 3000 ms. The dome and baffle pump openings are represented by wall segments 85 and 94 respectively.

To illustrate how the GTNEUT code can be used to test recycling hypotheses, the $\Gamma_{dome} / \Gamma_{baffle}$ ratio was calculated for uniform recycling from the main chamber wall (the second case in Table 1) and for various combinations of recycling flux ratios among the various regions near the divertor strike points. These results are shown in Table 1. It can be seen that the $\Gamma_{dome} / \Gamma_{baffle}$ ratio is a sensitive function of the location of the recycling source and perhaps could be used as a diagnostic of the recycling location.

Table 1: Sensitivity of the $\Gamma_{dome} / \Gamma_{baffle}$ ratio to various recycling assumptions. The total recycling source is kept constant for all cases and equal to 1.0×10^{23} #/s. Numerical subscripts correspond to the GTNEUT wall numbering scheme (see Fig. 1).

Flux distribution	Γ_{dome} **(#/s)**	Γ_{baffle} **(#/s)**	$\Gamma_{dome} / \Gamma_{baffle}$
$\Phi_{84} = \Phi_{86} = \Phi_{93} = \Phi_{95}$	0.5695×10^{22}	0.6426×10^{22}	**0.88**
Uniform (MCR)	0.613×10^{21}	0.71×10^{21}	**0.86**
$\Phi_{86} = \Phi_{93}$, $\Phi_{84} = \Phi_{95} = 0$	0.192×10^{22}	0.924×10^{22}	**0.20**
$\Phi_{86} = 1.5\times\Phi_{84}$ $\Phi_{93} = \Phi_{95}$	0.494×10^{22}	0.643×10^{22}	**0.76**
$\Phi_{in} / \Phi_{out} = 0.5$	0.380×10^{22}	0.855×10^{22}	**0.45**
$\Phi_{in} / \Phi_{out} = 2.0$	0.760×10^{22}	0.430×10^{22}	**1.77**

1. J. Mandrekas, R. J. Colchin, W. M. Stacey, et al., Nucl. Fusion, **43**, 314 (2003).

D. ROTATION

(J. Mandrekas and W. M. Stacey)

We have previously compiled[1] and successfully tested against DIII-D data[2] a neoclassical model for the calculation of plasma rotation and gyroviscous momentum transport. The calculation model consists of a coupled set of non-linear momentum balance equations for the toroidal and poloidal velocities and the sine and cosine components of the density asymmetry over the flux surface for each ion species present (2 in our present model). We have reviewed the derivation of these various equations to make field and current direction explicit in the formalism and to avoid making certain series expansions that could lead to inaccuracies under certain extreme conditions. We are now in the process of developing and testing robust solution procedures for this nonlinear set of equations.

This work was reported at APS-DPP-03.

1. W. M. Stacey, Phys. Plasmas, 8, 158 (2001).
2. W. M. Stacey and J. Mandrekas, Phys. Plasmas, 9, 1622 (2002).